Raptor-IRSA Grant-free Random Access Protocol for Smart Grids Applications

Angel Esteban Labrador Rivas, Taufik Abrão

Abstract

This paper deals with the reliability of random access (RA) protocols for massive wireless smart grid communication (m-SGC). We propose and analyze an improved grant-free RA (GF-RA) protocol for critical SG applications under strict QoS m-SGC requirements. At first, we discuss the main features of the SG neighborhood area network (NAN) architecture. We explore the main features of low-rate machine-type wireless networks, and also we describe a technology characterization of wireless neighborhood area networks (WNAN) in medium-range coverage applications. We propose a new-improved irregular repetition slotted ALOHA, combing Raptor codes and irregular ALOHA, namely RapIRSA random access protocol, to better respond to critical high-reliability QoS requirements under a 5G network perspective. Then, we compare and comprehensively analyze the proposed RapIRSA protocol with two existing RA protocols, the IRSA protocol, and the classical Slotted Aloha. Finally, We summarize the potential challenges in implementing the proposed RA protocol for SG critical applications considering many smart sensors (SS).

Index Terms

Smart grid; Random Access Protocols; Massive MTC; Quality of Service; Raptor codes.

I. INTRODUCTION

Most of the modern Smart Grids (SG) Quality of Service (QoS) models arrange a mapping method with an electrical-telecommunication design. The industry application experience and electrical engineering decisions rarely foresaw SG service requirements.

A. E. L. Rivas and T. Abrão are with the Electrical Engineering Department, State University of Londrina, PR, Brazil. Rod. Celso Garcia Cid - PR445, s/n, Campus Universitário, Po.Box 10.011. CEP: 86057-970. E-mail: angel.labrador@uel.br; taufik@uel.br

Wireless communications represent a challenge to SG implementation as many mission-critical applications require real-time data transfer. Maintaining delay and reliability SG requirements over wireless shared network disputes with the possibility to extend the number of sensor devices in a wireless network [1]. Also, wireless communications bring several security concerns for SG; authors in [1] explore techniques to improve the robustness of wireless mesh networks for mission-critical applications. As SG states as a cyber-physical grid with Internet-of-things (IoT) and 5G data acquisition integration multiple access emerges as trending research [2].

A *grant-based (GB)* scheduling operation guarantees that a user has restricted resources to the wireless channel, consequently circumventing unspecified collisions and increasing latency and communication overhead [3]. On the other hand, *grant-free (GF)* based Random Access (RA) protocols represent a solution to decrease the access latency [4]. GF-based protocols use transmission over shared resources if multiple neighboring users transmit simultaneously. Oversharing creates potential collisions that jeopardize transmission reliability. Currently, academic research and standardization commissions have proposed approaches to enhance the backed traffic loading with GF RA schemes while guaranteeing high reliability and low latency [5].

Several ALOHA-like schemes use successive interference cancellation (SIC) techniques to resolve multiple collided packets [6], [7], [8]. A certain number of time-slots compose the slotted-ALOHA (S-ALOHA) temporal frame where the user transmits a predefined number of times. Irregular repetition slotted ALOHA (IRSA) optimizes the probability mass function to maximize the peak throughput performance. IRSA performance results better than S-ALOHA and contention resolution diversity slotted ALOHA (CRDSA) [6], [9], [10], [11]. Furthermore, the number of time-slot adjustments relies on the base station (BS) tasks since transmission reaches the nominal throughput. Thus, a proper time-frame length avoids decay in the throughput performance.

A. Related Works

Recent literature addressing joint issues involving the problem of data collision, access delay, and/or power consumption in random access (RA) Internet of things (IoT) have been arising [12], [13], [14], and[15]. *E.g.,* a random access scheme for large-scale micro-power wireless IoT sensors based on *slot-scheduling and hybrid mode* has been proposed recently in [12]. This scheme is based on different time-slot structures, applying a specific slot-scheduling procedure according to network workload and power consumption. Sensors with

varying service priorities are arranged in other time slots for competitive access using an appropriate RA mechanism. Besides, the algorithm rationally places the number of time slots and competing devices into different time slots. This scheme can meet the timeliness requirements of different services and reduce the overall network power consumption when dealing with different RA scenarios, effectively reducing the overall power consumption. In contrast, high-priority services can meet the promptness requirements based on lower power consumption. Raptor-coded random access protocol to enable reliable transmission in the decentralized unmanned aerial vehicle (UAV) network is proposed in [13]. Since the considered network is composed of several overlapped RA interfering subsystems, the proposed Raptor-based RA scheme can reduce the bit-error rate (BER) by implementing three steps: *i*) selecting the number of time-slots based on a derived lower bound for reliable RA operation; *ii*) *error-correcting codes* are incorporated as precoding before RA operation; *iii*) by correlating two consecutive slots, an idle-slot-filling approach is aggregated to improve the RA system efficiency further. Numerical results reveal that the proposed 3-step strategy substantially reduces the BER while can save a substantial number of slots ($\approx 20\%$) compared with the existing frameless ALOHA scheme to attain a specific target BER. Several machine-type communication (MTC) random access devices can simultaneously transmit in the same resource block by incorporating Raptor codes, significantly reducing the access delay and improving the achievable system throughput [15]. A simple yet efficient random access strategy is proposed in [14], allowing both to detect the selected preambles and to estimate the number of devices that have chosen them. No device identification is needed in the RA phase, significantly reducing the signaling overhead. The maximum number of supported MTC devices in a resource block (RB) is characterized as a function of message length, available resources, and preambles. The proposed scheme can effectively support many MTC devices for a limited number of available resources when the message size is small.

Differently of [12], [13], [14] and [15], in this contribution, we deal with the challenges posed by wireless communications in the Smart Grids (SGs) scenarios and implementation, where many mission-critical applications require real-time data transfer. The challenge is maintaining the delay and reliability requirements in the SG over wireless shared network disputes, with the possibility to extend the number of sensor devices over the wireless network [1]. To overcome this challenge, industry application experience and engineering decision-makers must be considered in conceiving new methods under an electrical-telecommunication design approach, not only considering the power-energy design perspective. Moreover, wireless communications also bring several security concerns for SG systems; for instance, authors

in [1] explore techniques to improve the robustness of wireless mesh networks for mission-critical applications. As SG systems have been conceived as a cyber-physical grid with IoT and 5G data acquisition integration, multiple access communication schemes emerge as trending research inside the SG systems [2].

B. Contributions

The focus of this paper is to analyze the influence of GF-RA protocols in achieving QoS massive smart grid communication (m-SGC) requirements and propose a RA protocol for critical SG applications considering a massive number of Smart Sensor (SS). The main *contributions* of this work are threefold:

i) Elaborating on and proposing a new grant-free protocol that leverages Raptor codes and IRSA to improve the performance of RA protocols for SG applications. Our approach modifies the standard IRSA protocol by employing Raptor codes to reduce the number of preamble messages and the associated overhead while improving reliability and latency and adapting the protocol to account for different priority levels and varying numbers of devices in the network.

ii) Thoroughly characterizing the modifications required to adapt RA protocols to existing applications and varying numbers of devices in SG applications. Our work provides comprehensive guidance on the specific modifications required to ensure that RA protocols can achieve optimal performance and meet the QoS requirements of various SG applications.

iii) Exploring the QoS requirements of critical SG applications, such as AMI and load management, and characterizing the requirements of smart grid communication (SGC) systems to provide insights into the trade-offs and performance requirements of different RA protocols.

Overall, our proposed grant-free RA protocol, along with our detailed characterization of the necessary modifications and QoS requirements, represent a significant contribution to the field of SG communications and provides valuable insights into the design of RA protocols for m-SGC networks.

The remainder of the paper is organized as follows. The m-SGC schemes and applications are revisited in Section II. Random Access protocols suitable for m-SGC systems are considered in Section III, while Section IV describes important metrics deployed in the evaluation of QoS of SG systems. Section V introduces the proposed RA protocol. Extensive numerical results are explored in Section VI. Section VII draws the main conclusions and future trends.

II. M-SGC ARCHITECTURE AND APPLICATIONS

Smart grid (SG) applications have been implemented using various network technologies such as power line communication (PLC), wireless mesh networks, and low-power wide area networks (LPWAN) [16]. LPWAN has emerged as a popular technology for SG and smart city applications due to its long-range connectivity, low power consumption, and low cost [17]. LPWAN technologies such as LoRaWAN and Sigfox are particularly well-suited for SG applications because they can support many low-cost, low-power devices with infrequent data transmission [18]. Moreover, LPWAN enables the communication between devices that are located in hard-to-reach areas, such as underground or in remote locations [19]. These benefits make LPWAN an attractive choice for SG applications, particularly for use cases involving smart metering, distribution automation, and demand-side management [17].

In addition, one can note that SS and SG applications typically rely on IoT and various network technologies, including LPWAN [20], [21], [22]. These technologies play a significant role in meeting the evolving requirements of applications and services while providing a framework for enabling robust and dynamic solutions. However, LPWAN is not the only technology used for SG applications, and other network technologies such as PLC and wireless mesh networks have also been used [16].

Smart utility network (SUN) targets multiple applications within shared networks [23]. For a utility, this implies performing monitoring and control over the same resources. SUN devices provide wide-long-range point-to-point connections, including many outdoor devices. SUN aims for low-power wireless applications that usually demand the maximum transmit power available under proper administration. SUN application requirements demand a peer-to-peer topology [24]. In a star topology, devices establish communications with a single central controller, named the Neighborhood Area Network (NAN) coordinator. In contrast, each device in a peer-to-peer network can route messages among and through any device, making it more flexible for certain applications.

Most of the delay allowances discussed in this work are a compilation of the requirements specified in previous works [25], [26], [27], [28], [29]. In [30], the authors provide a quantitative characterization of priorities for SG applications based on these standards, recommendation documents, pragmatic needs for utility, and Table I includes the priority of an application relative to others. Besides, *delay* allowances listed in this table are end-to-end Uplink delays.

Note that the latency requirements for SUN applications may vary depending on the

specific use case and application. For example, some applications may require strict latency requirements to ensure proper operation, while others may be more tolerant of delay.

TABLE I: Latency & Priority by SG application type.

Application type	Latency (ms)	Priority 0-max 100-min
Teleprotection (60 Hz, 50 Hz)	8,10	10
SCADA	10	20
Teleprotection	16	15
Synchrophasors	20	12
SCADA	100	25
Distribution automation	100	26
Distributed generation - distributed storage	100	27
MWF	100	30
Business voice	200	60
Dynamic Line Rating	200	28
CCTV	200	55
SCADA, DA, DG/DS, DLR	200	45
Business data	250	70
AMI	250	40
Protection	500	80
Many/others	2000	100

This table shows only higher priority applications by application type (non-exhaustive)

A. Types of Frame in 5G Mobile networks

In smart grids, the design of wireless communication systems and protocols faces significant challenges due to the heterogeneity of prosumers, nodes that can consume and produce electrical power, and high reliability and latency requirements and data rates. Defining the technical requirements for smart grid applications, such as latency, rates, and reliability, remains an ongoing research area. Recent studies have shown that existing wireless communication technologies are insufficient to meet the stringent demands of a time-critical smart grid with strict requirements on latency [31]. The typical response time for different SG applications can be found in Table I. However, there are no specifications on latency for many

new scenarios of smart grid, such as nano-grids[1], which are supposed to have even higher technical standards when connected to main grids. In Table I, different instances of SCADA refer to different sub-types or use cases, such as transmission SCADA, distribution SCADA, and substation automation SCADA, each with unique latency and priority requirements.

The 5G systems have been developed for supporting various services, such as enhanced mobile broadband (eMBB), massive machine-type communication (mMTC), and ultra-reliable low-latency communication (URLLC). The latter two constitute IoT enablers. The high propagation loss in the above 3 GHz spectrum, the limited number of UL slots in a time-division duplexing (TDD) frame, and the limited user power strongly restrict the wireless communication coverage. Moreover, the stringent requirements of eMBB and IoT applications lead to 5G challenges, including site planning, ensuring seamless coverage, adapting the TDD DL/UL slot ratio, and the frame structure for maintaining a low BER, as well as low latency. Conflicting requirements of high-transmission efficiency × large coverage area × low latency can be balanced by properly exploiting the spectrum, enabling the IoT and eMBB services support.

New Radio (NR) *frame structure* is specified in 3GPP specification (38.211) [32]. 5G NR retains the concept of a 10-millisecond frame divided into ten one-millisecond subframes. There is also a slot concept, but its definition differs from a slot in LTE. One slot is defined as 14 OFDM symbols corresponding to once a frame or one millisecond in LTE frame legacy. A frame has a duration of 10 ms, which consists of 10 subframes having 1ms duration, each similar to LTE technology. Each subframe can support time slots of 2μs duration. Each slot typically consists of 14 OFDM symbols. The radio frame of 10 ms is transmitted continuously as per TDD topology, one after the other. A subframe is of fixed duration *i.e.* 1ms, whereas slot length varies based on subcarrier spacing and the number of slots per subframe. It is 1 ms for 15 KHz, 500 μs for 30 KHz, and so on. Subcarrier spacing of 15 KHz occupies 1 slot per subframe, subcarrier spacing of 30 KHz occupy 2 slots per subframe, and so on. Each slot occupies either 14 OFDM symbols or 12 OFDM symbols based on normal Cycle Prefix (CP) and extended CP respectively [33].

III. RA Protocols for Required QoS in m-SGC Networks

In this section, we define suitable network scenarios for RA protocol applied to m-SGC networks. We consider a cellular-based single-cell system with up to M total users connected

---

[1]SG in resident areas that may have complex nodes such as prosumers.

to the BS, where $m(t)$ users are active at any time occurrence t; or more specifically at the k-th time-slot, $m(\tau_k)$. Furthermore, a Beta or a Poisson distribution determined the distribution of the active users m (see Section III-B)..

A. ALOHA-*based Classical RA Protocol for SG systems*

ALOHA-based protocols are among the RA protocols group of high-reliability and high-throughput applications [34]. This work concentrates on extensions of the ALOHA model, holding terminals send a slotted packet over the channel as quickly as it is produced and without performing distributed coordination strategies.

In the sequence, we define the premises for evaluating the performance of the implemented/developed RA protocols in terms of two metrics. The first metric, *throughput* (S), summarizes the average amount of data blocks accomplished at the receiver over a reference period. The second is a complementary metric, the *packet loss ratio* (PLR), eq. (8).

1) Slotted ALOHA: Fig. 1 depicts a sketch of the slotted ALOHA and the IRSA RA protocols. n slots lasting T_F seconds build a frame F. The total number of active users is m. The MAC frame, also called Random Access Frame (RAF), of T_F duration, is composed of n slots of duration $t_\mathrm{s} = T_F/n$. In every MAC frame, a measurable number of users m try a packet transmission in a determined instant. Hence, in each MAC frame, each user performs a unique transmission associated with a new packet or the retransmission of a previous collision. Further, a MAC frame with a collision does not allow retransmission. The last statement will generate some back-logged users.

The *normalized offered traffic* (or network load) follows by:

$$G = \frac{m}{n} \qquad \left[\frac{\text{user}}{\text{slot}}\right] \tag{1}$$

Therefore, the *normalized throughput* (or channel output) S is characterized as the probability of successful packet transmission per slot, where n is the number of slots transmitted in T_F seconds. Fig. 1.(a) presents an S-ALOHA frame with individual packet transmission by MAC frame. Collisions drive retransmissions in the subsequent frame. Hence, the throughput for the S-ALOHA protocol can be defined as a function of normalized offered traffic:

$$S(G) = G \cdot e^{-G} \qquad \left[\frac{\text{packet}}{\text{slot}}\right] \tag{2}$$

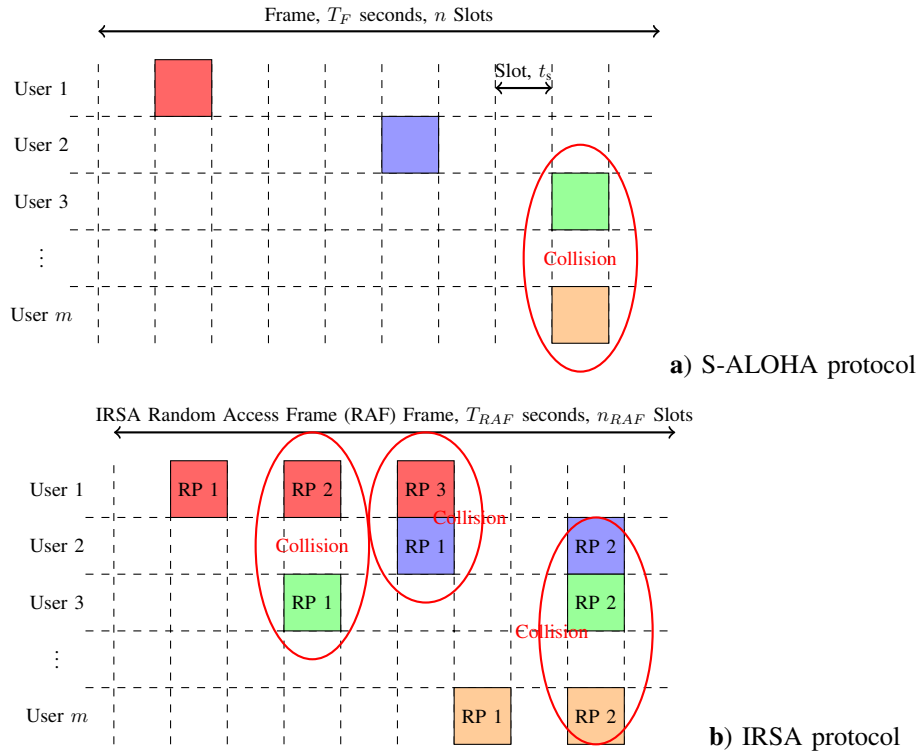where the peak throughput is attained at $S(1) = e^{-1} \approx 0.37$.

Fig. 1: Sketch of a) S-ALOHA; b) IRSA protocols as presented by [6]

2) The Upbound of 0.37 for Slotted ALOHA: The upbound of 0.37 for slotted ALOHA has been extensively studied in the literature. Kennedy and Miller were the first to analyze the hidden terminal problem in carrier sense multiple-access and propose the busy-tone solution in 1975 [35]. Daut and Shorey analyzed a random-access scheme for satellite networks and derived the upbound in 1981 [36]. Eklund and Rahelić further studied the multi-access performance of packet radio networks with slotted ALOHA in 1986 [37]. More recently, Huang and van der Schaar proposed a compressive sensing-based approach for efficient and reliable random access in machine-to-machine communications in 2015 [38]. Le and Poor developed a probabilistic method for medium access control in wireless networks and derived the upbound in 2019 [39]. In recent years, several papers have focused on analyzing throughput for massive machine-type communications [40], and applying mean-field game theory to distributed power control in wireless communication [41].

3) IRSA Protocol: The IRSA protocol relies on the repetition of each packet access strategy by MAC frame. In Fig. 1.b) each packet is transmitted d times in a MAC frame. The repetition rate d ranges from packet to packet based on a statistical distribution. Hence, we define the

user sampling degree distribution by:

$$\Lambda(x) = \sum_{d=1}^{d_{\mathrm{m}}} \Lambda_{\mathrm{d}} x^d, \quad \text{with} \quad \sum_{d=1}^{d_{\mathrm{m}}} \Lambda_{\mathrm{d}} = 1 \tag{3}$$

where $0 \leq \Lambda \leq 1$ and each transmitter independently sends the replicas within the n time slots composing the MAC frame. Random transmission slots contain a maximum of d_{m} replicas sent.

Each packet contains a header with an index with the location of its copy. After receiving a packet successfully, the BS extracts the index identifying the replica positions. When packet replicas collide, they are extracted from the signal received in the corresponding slot removing the interference contribution. This procedure allows decoding packets transmitted in the same slot.

B. Traffic Model, Time Arrival, and Time Instance

Machine-Type Communication (MTC) traffic patterns differ from those for Human-to-Human (H2H) traffic. Better traffic models prompt better management of shared network resources and guarantee QoS for many types of devices. 3GPP proposes a simple Poisson process to model different kinds of network access coordinated or uncoordinated machine-to-machine (M2M) traffic [42]. Consequently, different arrival rate λ dynamically depends on the channel and system scenarios. 5G system scenarios are compiled in [43].

3GPP Specification number 37.868 define Machine-to-machine (M2M) traffic types, including a load analysis for Smart Meters (SM), fleet management, and earthquake monitoring applications. The document embraces a SM service with metering data reports, in fixed time intervals, and the load control and alarm events occurring randomly, being modeled by Poisson processes. Table II compiles the two traffic models.

Then IRSA protocol design in [6] considers Poisson traffic, *i.e.*, constant mean arrival even in SS applications with a disrupted appearance. On the other hand, the traffic model in [44] considers the Beta distribution that implicitly requires a time-varying mean parameter, *i.e.*, this traffic model accounts for the non-stationarity arrivals. Hence, the arrival distribution of the M_v active users in SG applications can be modeled by a Poisson or Beta distributions [44], [45] depending on the stationarity or non-stationarity arrivals assumption. Typical but different behavior in terms of the number of user activation is found considering Poisson and Beta distribution, Fig. 2.

After starting, an IRSA frame does not permit seeking users. Each late-activated user must wait for a full-frame duration T_F. The existence of a waiting time T_W within two IRSA

TABLE II: 3GPP traffic models for MTC proposed in the 3GPP TR 37.868 document.

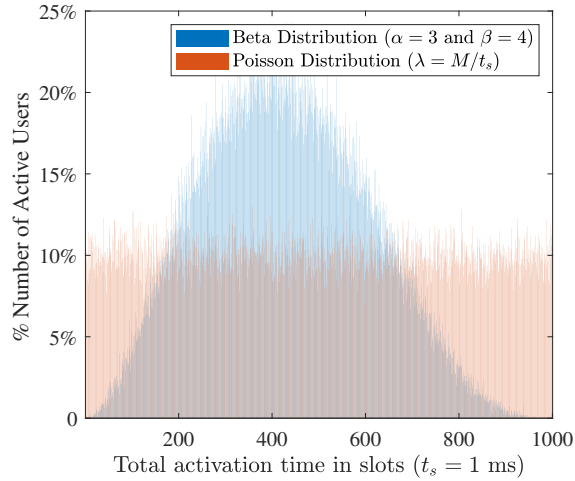| Parameter	Statistical Characterization
Traffic model 1	
Number of MTC devices	$M \in \{1000, 3000, 5000, 10000, 30000\}$
Arrival distribution	Uniform distribution over $T_A = 60$s
pk_s	200 bytes
Traffic model 2	
Number of MTC devices	$M \in \{1000, 3000, 5000, 10000, 30000\}$
Arrival distribution	Beta distribution over $T_A = 10$s
pk_s	200 bytes

Fig. 2: Users arrival in a Frame F with n time-slots considering Poisson $\times$ Beta distribution and $M = 100$ devices.

frames relies on latency limitations. Indeed the worst-case scenario implies a user decoded following the expiration of the IRSA frame.

Hereafter, the maximum latency Δ_i of the user i can be separated as

$$\Delta_i = T_W + 2T_F = T_{Ac} + T_F \leq \Delta_0 \tag{4}$$

A user's maximum latency should not exceed the latency constraint Δ_0. This scheme implies the accumulation of all users activated between IRSA frames.

C. Successive Interference Cancellation (SIC)

The scenarios involving M2M communications with smart sensors call for new ideas on RA schemes. The adoption of simple SIC technique makes it feasible to deliver throughput

enhancements in RA-based communication systems [46]. Based on the receiving and buffering MAC frame, the receiver looks for *singleton slots*, meaning slots with interference-free packets.

In the context of RA protocols, a graphical model can be described as an iterative SIC process [34], where the MAC frame standing through a bipartite graph $\mathcal{G} = (\mathcal{U}, \mathcal{S}, \mathcal{E})$ composed by three sets:

$\mathcal{U} = \{U_1, U_2, \ldots, U_m\}$ of m *user nodes* (UNs);

$\mathcal{S} = \{S_1, S_2, \ldots, S_n\}$ of n *slot nodes* (SNs);

$\mathcal{E} = $ *set of edges*.

The UN $U_i \in \mathcal{U}$ connects to the slot number (SN) $S_j \in \mathcal{S}$ by an edge $\mathcal{E}_{ij}$ conditioned to the copy of the ith packet of the ith user is transmitted in the jth slot. Fig. 3 depicts the graph illustration of a MAC frame with $n = 5$ slots and $m = 4$ users attempting a transmission. Notice that there is a 2-gather for users 1, 2, and 4, while user 3 packets repeat three times. One *singleton slot* for the received frame. A particular slot node has degree d if it is adjacent to d edges; for instance, in the example of Fig. 3, S_1 has degree $d = 2$, and that S_2 has degree $d = 1$.
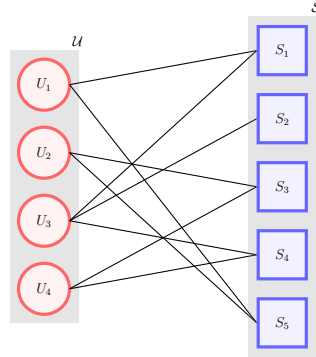

Fig. 3: Bipartite graph for a MAC frame with $n = 5$ slots and $m = 4$ users attempting a transmission

To model the SIC process through a graph, some simple rules must be applied. Iteratively, we search for SNs with degree $d = 1$. Estimate S_i to have degree 1, and indicate by U_j its only user node neighbor. Hence, we exclude the edges connected to S_i and U_j; equal to exclude the interference addition on the packet of user j in each transmitted slot. The SIC process repeats on the up-to-date graph. Following these rules, the SIC process applied to the example of Fig. 3 is sketched as a four canceling iterations process represented as graph model in Fig. 4.

(a) 1st iteration: S_2 has degree 1

(b) 2nd. iteration: S_1 and S_4 have degree 1

(c) 3rd iteration: S_5 has degree 1

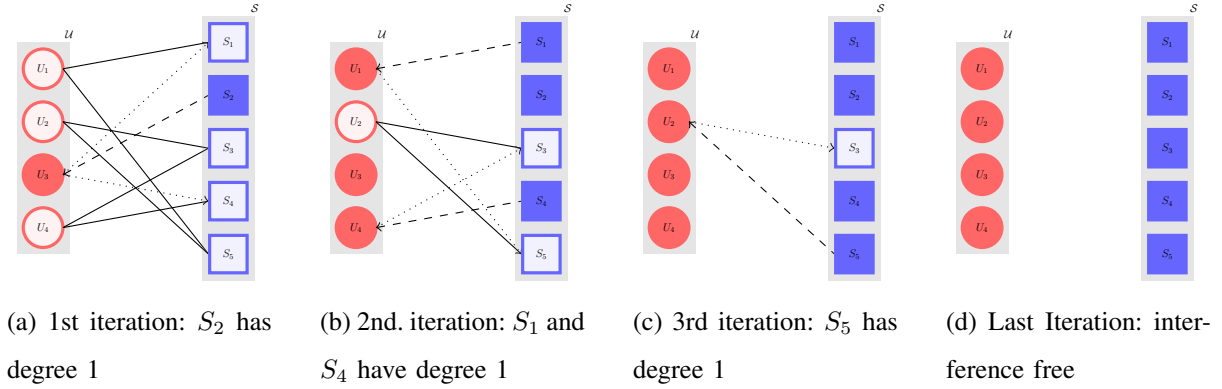(d) Last Iteration: interference free

Fig. 4: SIC decoding for the collision pattern of Fig. 3, tracked over the corresponding graph; four SIC iterations are represented.

The fundamental concept of SIC is decoding users' signal (devices) successively. After decoding one user, its signal is reconstructed and canceled from the total received signal before decoding the subsequent user's signal. In this work, we use the advantage of a singleton where at least one device is free of interference. Hence, assuming conventional SIC application, one of the users (strongest sinal), say S_1, is decoded treating $S_2, S_3, \ldots, S_n$ as interference. Next, the second strongest user' signal, S_2, is decoded by using the extracted, reconstructed, and subtracted S_1 signal from the total received signal. The canceling process is repeated until the last interfering signal is decoded. SIC implementation represents an advantage compared to the conventional decoding process, which treats all the interfering users' signals as noise.

D. Time-domain Structure

The parameters of SG system considered herein are based on the 5G NR standard [47], [32]. Time-domain NR transmissions take place into 10 ms length frames. The radio frame of 10 ms has transmitted continuously as per TDD topology. Each frame contains 10 equally sized subframes of duration 1 ms. Subcarrier-Spacing (ScS) establishes the bandwidth of each frame (BW_F) and the number of slots in a subframe. With slot-based scheduling, a slot is a minimum measure with a duration of t_s seconds. A subframe is of fixed duration *i.e.* 1ms, whereas *slot length* varies based on subcarrier spacing and the number of slots per subframe. It is 1 ms for 15 KHz, 500 μs for 30 KHz, and so on. Subcarrier spacing of 15 KHz occupies 1 slot per subframe, subcarrier spacing of 30 KHz occupy 2 slots per subframe, and so on. Finally, this work does not use a symbol-level scheduling technique.

IV. Metrics and Definitions in SG QoS

A. Latency

From the power system perspective, the latency requirement depends on the cycle of the electrical utility cycle ($T = 1/f$) to keep the stable stage of a wave. Generically, in the context of a smart grid, we define data (or message) latency as the time between a state's occurrence and an application's activation [48]. Each application has its own latency requirements depending upon the kind of system response it is dealing with. Besides, among the other delays, *communication delay* also adds to the latency and needs to be minimized.

The total delay on the communication network comprises propagation delays, transmission delays, queuing delays, and processing delays. Primarily, *latency* (L) represented by:

$$L = \tau \frac{1}{f} \tag{5}$$

where τ is the delay factor (in cycles). Real-time scale SG network considers short/small values of τ.

We define in the following the QoS metrics RA-related to SG applications: the latency of message, Packet Delivery Rate (PDR) reliability, and critical latency response.

1) Latency in SG Message: This work focuses on applications with communication latency performance as a priority and does not accept outdated data. Thus, we define the hard delay metric in the subsequent outlines.

Definition 1. *(Hard delay, HD) Application with a hard delay requirement turns useless if its delay passes the QoS requirement even in successful message delivery.*

Next, the delay requirement τ_{req} includes the required network bandwidth as:

$$BW_{\text{req}} = S \left(8\frac{\text{bits}}{\text{byte}}\right) \frac{1}{\tau_{\text{req}}} M \qquad [\text{bits} \cdot \text{Hz}] \tag{6}$$

where S and M are the service's data size in bytes, and the number of users, respectively.

B. Packet Delivery Ratio (PDR) and Packet Loss Ratio (PLR)

Definition 2. *Packet Delivery Ratio (PDR) represents the proportion of the total number of packets received by the data collector unit (DCU) successfully, P_{R}, to the total number of packets generated by the SG source nodes, P_G:*

$$PDR = \frac{\sum_{i=1}^{M} P_{R_i}}{\sum_{i=1}^{M} P_{G_i}} = \frac{P_R}{P_G} \tag{7}$$

Definition 3. *Packet Loss Ratio (PLR) is a matched metric to the PDR defined as the probability for a user incorrectly decoded at the receiver after accessed the channel. Using eq. (7) one can obtain an approximate expression for PLR:*

$$PLR = 1 - PDR = 1 - \frac{P_R}{P_G} \tag{8}$$

C. Reliability

A conventional reliability definition in computer systems deliver SG network reliability metric [49]. Network reliability counts the probability of a system achieving its services accordingly in a specified time duration. Accordingly, we define the *reliability factor* in the SG network context as:

Definition 4. *(Reliability, $\mathcal{R}$) The network reliability stands as the probability of succeeding in delivering a message to the destinations node (related to the PDR metric) within the maximum latency requirement. The reliability decreases when the message arrives after the delay requirement. SG network reliability under HD definition, $\tau_{HD_{\text{req}}}$ can be defined as follows.*

$$\mathcal{R}(\tau) = \begin{cases} PDR = 1 - PLR & \tau \leq \tau_{HD_{\text{req}}} \\ 0 & \tau > \tau_{HD_{\text{req}}} \end{cases} \tag{9}$$

Notice that in *ultra-reliable and low latency communications* (URLLC), a generic reliability requirement of $\mathcal{R} = 1 - 10^{-5}$ (*i.e.*, 0.99999) is required with the user-plane radio-latency of 1 ms for a single transmission of a 32-byte long packet.

Definition 5. *Application Complying Ratio (ACR). We introduce a new concept named ACR that represents the number of users to successfully comply with the Up-Link (UL) connection within delay requirements $\tau_{HD_{\text{req}}}$. In the context of SG applications, the ACR reliability can be defined by the sum of ratios along the N slots:*

$$\mathcal{R}_{ACR} = \frac{1}{N} \sum_{k=1}^{N} \frac{m(\tau_k)}{m_k} \tag{10}$$

where m_k is the number of total active users in the k-th time-slot, and $m(\tau_k)$ represents the number of users that effectively sent a packet at the kth time-slot $k \in \{1, \ldots, N\}$ within the latency requirement time, i.e., $\tau_k \leq \tau_{\text{req}_i}$. Such reliability metric quantifies the proportion of active users who succeed in sending a packet at the kth time-slot within the latency requirement time along N slots.

In eq. (10), the QoS metric allows to track specific application problems. Under specific protocol applications, the ACR reliability metric quantifies the trusted network data delivery.

V. PROPOSED RA PROTOCOL BASED ON RAPTOR CODES FOR M-SGC NETWORKS

In this section, we propose a new RA protocol to achieve higher throughput under over-loaded networks using additional nodes working as precoding of Raptor codes. This Raptor code implementation uses a subclass of the bipartite graph described in [50], [51].

Considering SG scenarios, in the sequel we describe briefly the Raptor codes, including their characteristics, advantages, and some application environments with the associated parameters. Then, we propose a modification in the traditional IRSA protocol, mainly in the values of the operational parameters and in the substructure of the protocol, depending on the application requirements, aiming at enhancing the protocol reliability suitable for *ultra-reliable low-latency communications* (URLLC) and *machine-type communications* (MTC) services. We label QoS information into active users preamble. This information adjusts the IRSA protocol to achieve QoS requirements.

A. Raptor Codes

Raptor codes (RapC) are a class of forward error correction codes that can provide reliable and efficient data transmission over unreliable communication channels [52]. These codes were introduced by A. Shokrollahi in 2003 [51]. RapC can be used to efficiently encode and decode data packets for transmission over noisy channels. They are based on the concept of fountain codes and use an iterative decoding process to recover the original data. RapC's *advantages* over traditional error correction codes include bandwidth efficiency, higher reliability, and less decoding complexity. RapC can also adapt to different channel conditions and can handle varying levels of noise and interference. Raptor codes have been widely used in various communication systems, including wireless networks, multimedia transmission, and satellite communications. In 5G mobile networks, Raptor codes are used in the control plane and user plane to improve reliability and reduce latency [53].

The key parameters involved in RapC include the degree distribution, symbol size, and encoding rate. The *degree distribution* determines the distribution of probability for the number of times each symbol appears in the code word. The *symbol size* refers to the size of the symbols in the code word. The *encoding rate* determines the ratio of the output code length to the input message length. The encoding process of Raptor codes is based on a Fountain code, which generates a potentially infinite number of encoded packets from

a source packet [54]. A decoder can recover the original message from a subset of these encoded packets. The *repetition rate* of Raptor code, *i.e.*, the number of times a message is encoded into the code is denoted by η. Raptor codes have been used in various application environments, including satellite and wireless networks [55], [56]. In the RapIRSA protocol, the *number of connecting nodes* ($c\mathcal{N}$) used is denoted by q [57].

Overall, Raptor codes are a powerful tool for providing reliable and efficient data transmission in various communication systems and channel scenarios. Their adaptability, high reliability, and low decoding complexity make them an attractive option for 5G mobile networks and beyond.

B. Combining Raptor Codes and IRSA (RapIRSA)

We consider m active users sending packets to BS or DCU. Some users will send packets via *connecting nodes* ($c\mathcal{N}$). All $c\mathcal{N}$ are placed equitably reaching many possible directly visible users. Each $c\mathcal{N}$ uses the Decode-and-Forward (DF) protocol to deliver the information to the BS. $c\mathcal{N}$ has less probability of packet collisions compared to BS because $c\mathcal{N}$ only received packets of data from connected users.

Fig. 5 illustrates the Raptor codes-structured (RapC) wireless networks. This follows a bipartite graph model illustrated in Fig. 3. Besides, $c\mathcal{N}$ represented by dark circles in a separated time slot; m represents the number of active users, n_{RapC} is the number of slot nodes (SN) in the frame, and $q = \lfloor \eta \cdot n_{\mathrm{RAF}} \rfloor$ is the number of $c\mathcal{N}$. Besides, n_{RapC} contains two elements, as n_{RAF} for SN of RAF, and n_q for SN of $c\mathcal{N}$s. Hence, the total SN is defined as:

$$n_{\mathrm{RapC}} = n_{\mathrm{RAF}} + n_q \tag{11}$$

Besides, the normalized offered traffic G for the RapIRSA follows the definition in Eq. (1).

In the example of Fig. 5, five users $\mathcal{U} = \{U_1, U_2, \dots, U_5\}$ and two $c\mathcal{N} = \{c\mathcal{N}_1, c\mathcal{N}_2\}$ have been considered. Connecting nodes $c\mathcal{N}$ do not have prior information about users' messages. After receiving data from neighboring devices they decode-and-forward (DF) the messages to the BS for final processing. $c\mathcal{N}_1$ decodes one packet from U_1 and U_5, and then forward the first decoded packet to the BS. Likewise, $c\mathcal{N}_2$ receives packets from U_2 and U_3, it decodes one packet, and then forwards the decoded packets to BS. Fig. 5 represents RapC with $\eta = \frac{1}{7}$ and $q = 2$, *i.e.*, the parameters RapIRSA(η, q) stand for the fraction of the number of IRSA random access frame[2] (RAF) length and the number of connecting nodes ($c\mathcal{N}$), respectively.
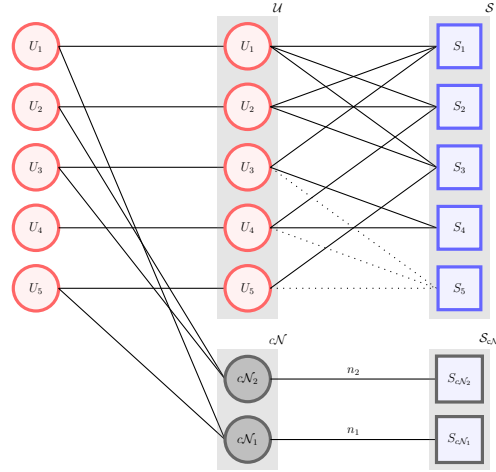
---

[2]Namely repetition rate of Raptor code.

Fig. 5: Raptor codes-structured wireless networks. RapIRSA(η, q) parameters: $\eta = \frac{1}{7}$ and $q = 2$.

In the Raptor codes-based RapIRSA scheme, $c\mathcal{N}_1$ and $c\mathcal{N}_2$ do not have prior information about the messages transmitted by users. They receive packets from neighboring devices and decode and forward (DF) them to the BS for final processing. In the case of collisions, the RapC enable them to decode as much information as possible from the received packets, even if the packets are partially corrupted due to collisions. Moreover, efficient decoding algorithms such as belief propagation or message passing can be used at the connecting nodes to mitigate the effect of collisions and improve decoding performance. Recent research has shown the effectiveness of such algorithms in dealing with collisions in various wireless communication scenarios [58], [59].

1) Practicability: The proposed RapIRSA scheme requires each random access node to transmit its packet to three nodes (BS, $c\mathcal{N}_1$, and $c\mathcal{N}_2$). However, we believe that the proposed method is practical in real-world wireless network scenarios. The transmission scheme used in RapIRSA is similar to that used in other existing schemes such as CRDSA, which has been shown to be practical and effective in different network scenarios [60], [61]. Furthermore, RapC used in our proposed scheme has been shown to improve reliability and reduce overhead in several other contexts of application [51], [62]. Moreover, our proposed RapIRSA scheme is designed to be scalable and flexible to accommodate different numbers of users and connecting nodes. Efficient algorithms such as *belief propagation* or *message passing* can be used for the decoding process at the connecting nodes [63]. Therefore, we believe that our proposed RapIRSA scheme is practical and can be implemented in various real-world scenarios.

Fig. 6 depicts the time-slot structure including the RAF implemented in the IRSA protocol and the slots with information from the $c\mathcal{N}$s. BS uses pre-coding through $c\mathcal{N}$s to detect failing nodes during the contention period. As discussed in the numerical results, Section VI, the Combining Raptor Codes and IRSA (RapIRSA) protocol is able to improve throughput performance substantially under high network load configurations, *i.e.*, $G > 0.6$.
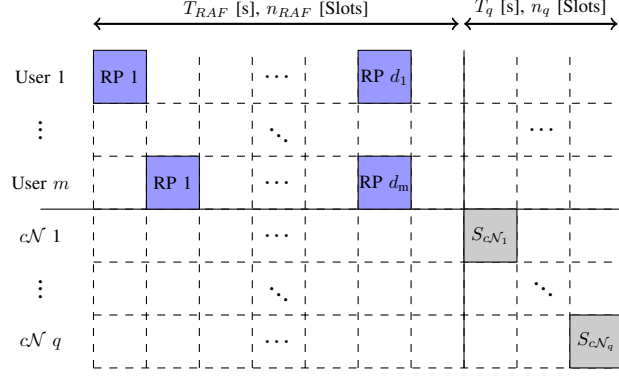

Fig. 6: Overview of RapIRSA time-slots structure.

The pseudo-code for the adopted graph-based decoding algorithm is described in the Algorithm 1. Moreover, Fig. 7 depicts an additional graph from BS $\mathcal{G}_{\text{BS}}$ and two $c\mathcal{N}$s ($\mathcal{G}_{c\mathcal{N}_1}$ and $\mathcal{G}_{c\mathcal{N}_2}$) seen by DCU.

Algorithm 1: Network Decoding with RapC

Data: Connected bipartite graphs $\mathcal{G}_{\text{BS}}$ and $\mathcal{G}_{c\mathcal{N}_j}$.

Result: Information m decoded.

for $j = 1$ *until* q **do**

    Loop Passive Nodes $\mathcal{G}_{c\mathcal{N}_j}$**:** Analyze $\mathcal{G}_{c\mathcal{N}_j}$ and access user U_i connected to a slot node having degree $d = 1$; **if** *degree* $d = 1$ **then**

        Obtain information of U_i ;

        Deduct the collected signals in all slot nodes correlated to user U_i with user U_i's information at graph $\mathcal{G}_{c\mathcal{N}_j}$;

        Send information of U_i via $S_{c\mathcal{N}_j}$ and deduct all slot nodes correlated to user U_i at graph $\mathcal{G}_{\text{BS}}$;

    end

end

Loop BS $\mathcal{G}_{\text{BS}}$**:** Implement SIC decoding algorithm as describe in Section III-C;

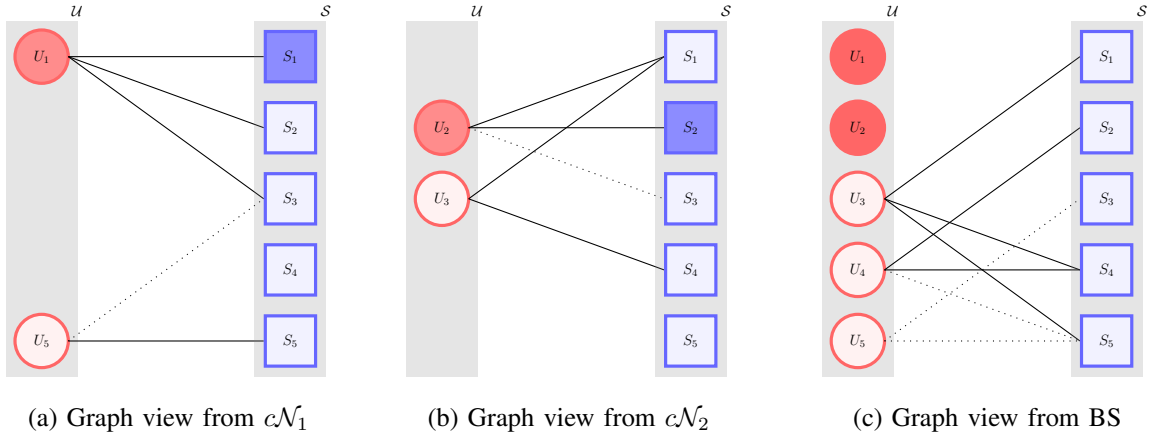(a) Graph view from $c\mathcal{N}_1$ (b) Graph view from $c\mathcal{N}_2$ (c) Graph view from BS

Fig. 7: Bipartite graphs-based message decoding received from the main links $\mathcal{G}_M$, connecting node $c\mathcal{N}_1$, and $c\mathcal{N}_2$.

SP-IRSA & SP-RapIRSA. Service Priority-based Irregular Repetition Slotted ALOHA (SP-IRSA) and Service Priority-based Raptor Code Irregular Repetition Slotted ALOHA (SP-RapIRSA) protocols employ additional preamble information to denote the number of packets in the channel, thus the high priority services have higher repetition probability. Such approach based on service priority does not consider the access probabilities adjusted according to the traffic load as Irregular Repetition Slotted ALOHA with Priority (P-IRSA) [64], which requires a further access controller. SP-IRSA protocol arranges m users into P_L different priority levels based on service-defined priority. Each user carrier services ID to determine whether repetition rate changes according to priority. The categorical priority level vector $\boldsymbol{p}_L$ increases (or decreases) the repetition probability of Λ_d. With a finite number of SG applications, the level P_L of each service modifies the maximum of d_m replicas a user m could send. Consequently, a user with a higher-level priority sends more replicas of its packet.

SP-S-ALOHA. Following the SP-IRSA description, we have implemented the same Service Priority-based on the S-ALOHA algorithm, namely SP-S-ALOHA. In this case, the service priority modifies the backoff maximum value in the user connection. Whether if the back-logged active users no comply in the attempt, the QoS system counts as an error, *i.e.*, in the worst-case scenario where backoff value is close to the maximum service priority, the user only will have an attempt to complete the uplink connection.

VI. NUMERICAL RESULTS

In this section, we present the simulation results of the proposed service priority RA algorithms based on S-ALOHA, IRSA, and RapIRSA protocols. The simulation process directly

follows the SG RA protocols revisited in Section III, as well as the proposed RA algorithms for m-SGC networks described in Section V. All the simulations use the MATLAB and JULIA programming languages. The main parameter values adopted in numerical simulations are summarized in Table III. We consider a future AMI scenario of SG networks, an urban area with up to 10^6 SM uniformly distributed in a 1×1 km service area. The coordinator node is center-located, and the $c\mathcal{N}$s, corresponding to the RapIRSA protocols are located to access as many as possible different devices.

TABLE III: Simulation Parameters

Parameter	Value
Service Area	$A = 1\text{km}^2$
# Active users, m	Up to $M = 10^6$ devices
Network Load	$G = \frac{m}{n} \in \,]0;\,1.2]\ \left[\frac{\text{user}}{\text{slot}}\right]$
Active Users distribution	Poisson & Beta
Time-slot duration	1 ms
IRSA RAF Length	$n_{\text{RAF}} = 50\ slots$
# Replicas (Max.)	$d_{\text{m}} = 8$
Degree distribution	$\Lambda_8(x) = 0.5x^2 + 0.28x^3 + 0.22x^8$
# SIC iterations (Max.)	$\mathcal{I} = 20$
S-ALOHA Back-off limit	$B_{\text{off}} = 50\ slots$
number of $c\mathcal{N}$	$q = \begin{bmatrix} 2 & 3 & 8 \end{bmatrix}$
fraction of n_{RapC}	$\eta = 0.25$
# SP m Users	Up to $M = 10^4$ devices
Priority Level	$\boldsymbol{p}_L = [0(\text{max}) \quad 100(\text{min})]$
# Realizations	100
Simulation time	10 s

Fig. 8 depicts the throughput for S-ALOHA (SA), IRSA, RapIRSA$(0.25, 8)$, and RapIRSA$(0.25, 2)$ implementations for two different users' arrival distributions. This simulation includes the theoretical throughput for S-ALOHA algorithm considering the Poisson distribution and an asymptotic ($n_{\text{RAF}} \to \infty$) representation of the IRSA protocol. Note that RapIRSA improved throughput not only for $G > 1$ but its performance is also comparable with the asymptotic IRSA with the Poisson distribution. It's worth mentioning, RapIRSA for $G > 1.4$ present a better throughput under traffic governed by a Beta distribution. In our specific scenario, this finding represents a breakthrough to determine that the RapIRSA protocol attains better performance operating under overloaded networks.

Accordingly, Fig. 9 depicts the packet loss ratio versus the network load. Under low and moderate-to-high network loading condition, *i.e.*, $0 < G < 1.2$ (Poisson distribution) and
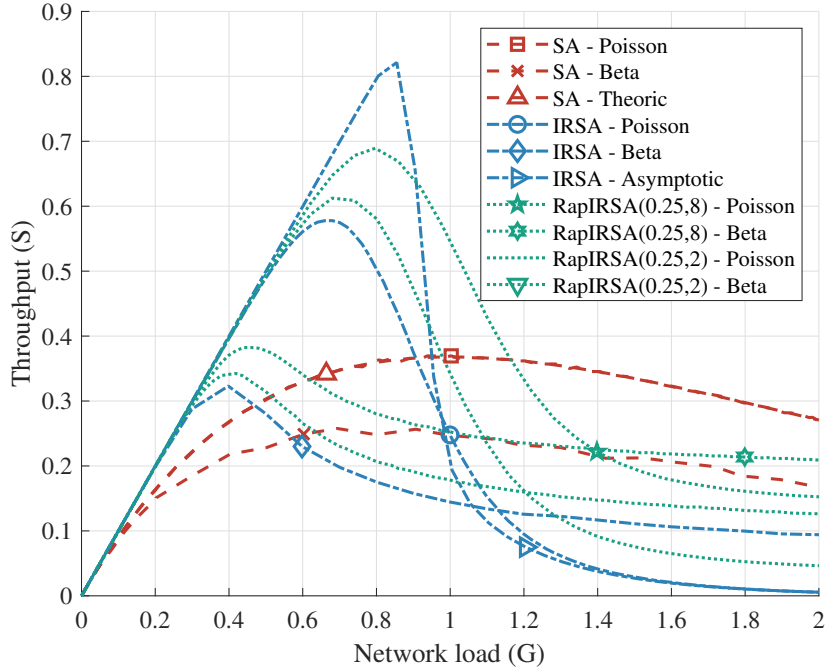
Fig. 8: Simulated throughput for SA, and for IRSA and RapIRSA with $\Lambda_8(x)$.

$0 < G < 0.6$ (Beta distribution), those values indicate a considerable advantage from IRSA and RapIRSA over S-ALOHA protocol, considering both arrival distributions. $\Lambda_8(x)$ is a commonly used degree distribution in the literature for modeling various types of networks, including communication networks and power grids. It is a power law distribution, which means that it has a heavy tail that captures the presence of a small number of highly connected nodes in the network. This makes it a suitable choice for modeling networks with heterogeneous connectivity patterns, such as smart grid networks. Moreover, the choice of $\Lambda_8(x)$ is consistent with previous work on modeling smart grid networks, which has also used power law degree distributions [65], [66].

A. Latency

When we first introduced Fig. 6 the extra slots n_q for each frame in the RapIRSA protocol, it creates concern about increasing latency. As delay constraints are fundamental to achieve QoS requirements, an additional evaluation of these parameters is presented in Fig. 10 to chart those values within IRSA and SA protocols. Fig. 10 shows that the *average delay* [slots] (red curves) and the associated *average delay* [slots/active users] (blue curves), for all investigated algorithms. Hence, as network loading increases, S-ALOHA maintains a steadily increasing behavior, resulting in high delays (over 10^5 slots) over high network loading ranging from $1 < G < 2$. Moreover, the IRSA protocol presents a remarkable performance without delay
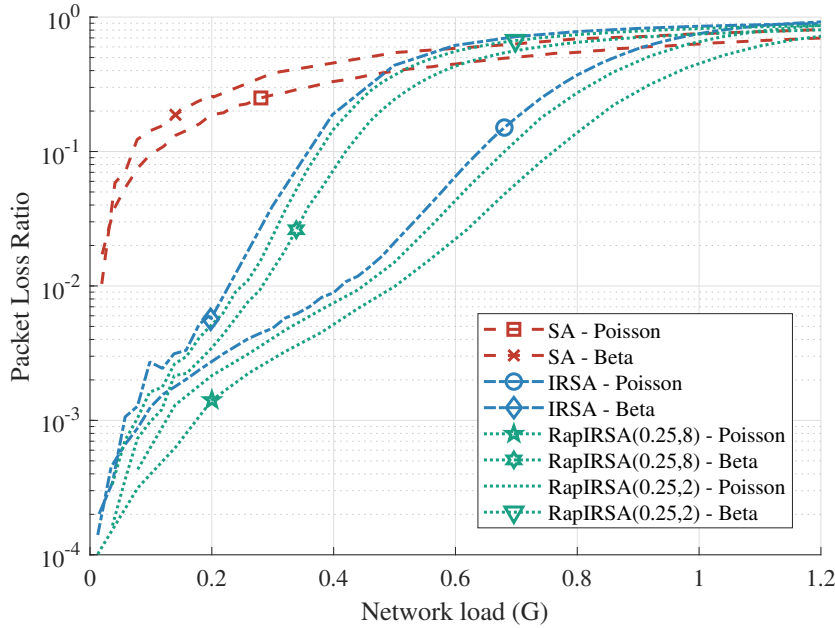
Fig. 9: Packet loss ratio for SA, and for IRSA with $\Lambda_8 = 0.5x^2 + 0.28x^3 + 0.22x^8$.

for low-medium network loading ($G < 0.5$). Furthermore, RapIRSA keeps an almost constant operation point for all network loading. Even for measurement of the average delay (slots) per active users in Fig. 10 (right y-axis), the delays of the S-ALOHA protocol appear unfeasible under requirements described in Table I for many of the SG applications. Table I scales priority in SG application type based on maximum tolerable latency.

B. Application Complying Ratio (ACR) Reliability

Fig. 11 compares the percentage of ACR reliability to evaluate the RA algorithm capability in achieving a certain QoS requirement. Under such specific reliability metric, and the modifications in the IRSA protocol introduced in Sec. V, which are based on Raptor codes deployment and service priority, the QoS information was labeled into the active user's preamble. The ACR reliability metric is evaluated with up to 10^4 devices; all SP RA protocols discussed in this work use the p_L values described in Table I. The ACR reliability curves in Fig. 11 corroborate the viability of the proposed RapIRSA and SP-RapIRSA algorithms to improve RA protocols performance, as well as, reach QoS requirements, described as one of the main objectives of the proposed work. Both RapIRSA variants, SP-RapIRSA and RapIRSA, provide the best ACR values across the entire networking loading range. Moreover, Fig. 11 reveals that the critical scenario of 90% ACR reliability ($\mathcal{R}_{\text{ACR}} = 0.9$), is attained for different network loading, depending of which RA protocol is adopted; the best performance is achieved by the SP-RapIRSA for a network loading of $G = 0.2$, followed by the RapIRSA
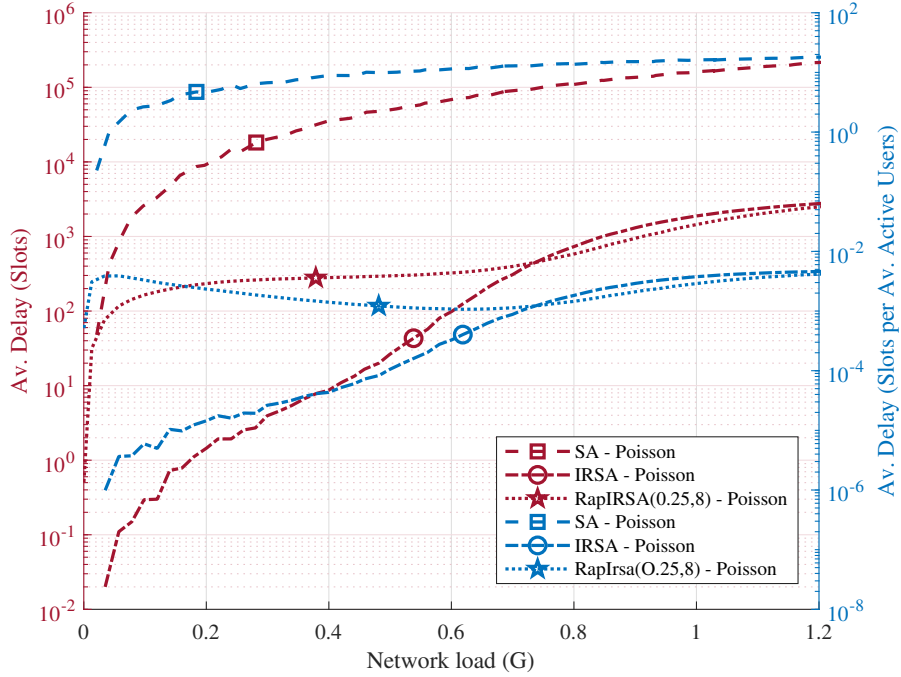
Fig. 10: Average delay in terms of # slots (left y-axis) and # slots per average # active users (right y-axis) *vs* Network loading.

protocol. The ACR reliability metric reveals the crucial trade-off between a delivered packet within the latency constraints. Notice that promising RA protocols for m-SGC applications require considering carefully the ACR reliability constraint.

Combining the superior ACR performance depicted in Fig. 11 with the reduced packet loss ratio (Fig. 9), balanced delay *vs.* network load in Fig. 10, and suitable throughput (Fig. 8) attained by the RapIRSA protocol, one can infer that among the three GF RA protocols analyzed, the RapIRSA is promising and the most feasible protocol for SG applications. Even with the addition of extra slots for the $c\mathcal{N}$ delays, RapIRSA can comply with tied throughput, PLR, and latency performance requirements in the current SG networks.

C. Computational Load and Memory Requirements

The computational load and memory requirements imposed by the proposed RA algorithms are evaluated by simulations performed on a workstation with an Intel Core i7-10700K CPU, 3.70GHz, and 16GB of RAM. Table IV summarizes the computational load in terms of the average processing time per packet and memory requirements of the RA algorithms. The *processing time* was measured for the analyzed RA algorithms based on S-ALOHA, IRSA, and RapIRSA protocols, respectively. The computational load of the proposed RA algorithms based on IRSA and RapIRSA protocols is substantially higher than the S-ALOHA
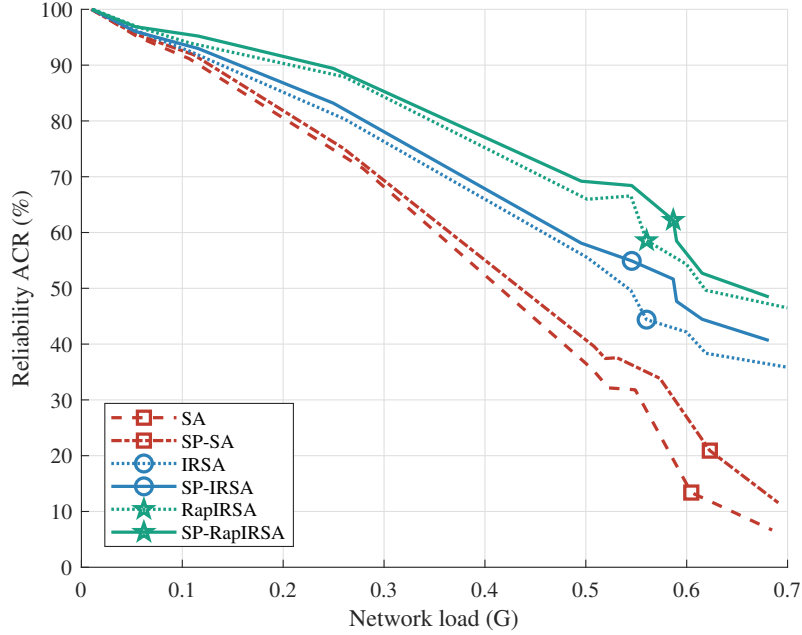
Fig. 11: Application complying rate (%) to measure algorithm capability to achieve QoS requirement.

protocol. Specifically, the RapIRSA presents a higher computational load than IRSA due to the additional processing time required for the encoding and decoding process of Raptor codes. However, the difference in processing time is negligible for a single packet. The memory requirement of the proposed RA algorithms is also presented in Table IV. As expected, the memory requirement of the RapIRSA protocol is higher than IRSA ($2\times$) and S-ALOHA ($20\times$) due to the additional storage requirement for encoded packets.

TABLE IV: Computational Load and Memory Requirements of RA Algorithms.

RA Algorithm	Avg. Processing Time/Packet (ms)	Memory Requirement (KB)
S-ALOHA	0.1	1
IRSA	0.5	10
RapIRSA	0.6	20

Overall, the proposed IRSA and RapIRSA RA algorithms require higher computational load and memory compared to the S-ALOHA protocol. However, considering the higher reliability and lower packet loss rate achieved by the proposed RA algorithms, the additional computational load and memory requirement can be justified, both attaining improvements in the performance-complexity trade-off. Finally, the computational load and memory require-

ment of both RA protocols can be further optimized by employing efficient encoding and decoding techniques for Raptor codes.

VII. CONCLUSIONS

We propose a service priority RA protocol for SG communication network applications. The proposed algorithm is based on the S-ALOHA and IRSA RA protocols with adapting parameters considering the QoS requirements as priority, latency, and data rates metrics. The proposed protocol aims to enhance the probability of success of various SG applications.

The RapIRSA protocol is proposed in this paper to guarantee better throughput of active users with the help of connecting nodes ($c\mathcal{N}$). We have shown that relative to SA and IRSA in particular for multipacket messages, the RapIRSA can increase the reliability and keep the throughput above all others. The RapIRSA is better than SA and IRSA, indicating this protocol is suitable for SG applications.

The investigation of adapting IRSA & RapIRSA for smart sensors' future applications can be guided by the following issues and findings: **a**) such protocols reach their peak performance without latency constraints; **b**) they rely on reliability constraints rather than latency constraints; **c**) latency constraints on IRSA & RapIRSA depend on the limit of the frame size; nevertheless, a decreasing frame size supports fewer users, rejecting some users from the system; **d**) IRSA & RapIRSA represent acceptable solutions for many critical applications.

REFERENCES

[1] H. Khalid and A. Shobole, "Existing Developments in Adaptive Smart Grid Protection: A Review," *Electric Power Systems Research*, vol. 191, no. September 2020, p. 106901, feb 2021. [Online]. Available: https://doi.org/10.1016/j.epsr.2020.106901https://linkinghub.elsevier.com/retrieve/pii/S0378779620306994

[2] H. Shahinzadeh, A.-s. Mirhedayati, M. Shaneh, H. Nafisi, G. B. Gharehpetian, and J. Moradi, "Role of joint 5g-iot framework for smart grid interoperability enhancement," in *2020 15th International Conference on Protection and Automation of Power Systems (IPAPS)*, 2020, pp. 12–18.

[3] Y. Liu, Y. Deng, M. Elkashlan, A. Nallanathan, and G. K. Karagiannidis, "Analyzing Grant-Free Access for URLLC Service," *IEEE Journal on Selected Areas in Communications*, vol. 39, no. 3, pp. 741–755, mar 2021. [Online]. Available: https://ieeexplore.ieee.org/document/9174916/

[4] G. Berardinelli, N. Huda Mahmood, R. Abreu, T. Jacobsen, K. Pedersen, I. Z. Kovacs, and P. Mogensen, "Reliability Analysis of Uplink Grant-Free Transmission Over Shared Resources," *IEEE Access*, vol. 6, pp. 23 602–23 611, 2018. [Online]. Available: https://ieeexplore.ieee.org/document/8340053/

[5] E. Recayte, A. Munari, and F. Clazzer, "Grant-Free Access: Machine Learning for Detection of Short Packets," in *2020 10th Advanced Satellite Multimedia Systems Conference and the 16th Signal Processing for Space Communications Workshop (ASMS/SPSC)*. IEEE, oct 2020, pp. 1–7. [Online]. Available: https://ieeexplore.ieee.org/document/9268917/

[6] G. Liva, "Graph-Based Analysis and Optimization of Contention Resolution Diversity Slotted ALOHA," *IEEE Transactions on Communications*, vol. 59, no. 2, pp. 477–487, feb 2011. [Online]. Available: http://ieeexplore.ieee.org/document/5668922/

[7] M. Oinaga, S. Ogata, and K. Ishibashi, "Received-Power-Aware Frameless ALOHA for Grant-Free Non-Orthogonal Multiple Access," in *2020 International Conference on Information Networking (ICOIN)*, vol. 2020-Janua. IEEE, jan 2020, pp. 282–285. [Online]. Available: https://ieeexplore.ieee.org/document/9016466/

[8] Y.-C. Huang, S.-L. Shieh, Y.-P. Hsu, and H.-P. Cheng, "Iterative Collision Resolution for Slotted ALOHA with NOMA for Heterogeneous Devices," *IEEE Transactions on Communications*, vol. 6778, no. c, pp. 1–1, 2021. [Online]. Available: https://ieeexplore.ieee.org/document/9354838/

[9] A. Munari and A. Frolov, "Average Age of Information of Irregular Repetition Slotted ALOHA," in *GLOBECOM 2020 - 2020 IEEE Global Communications Conference*. IEEE, dec 2020, pp. 1–6. [Online]. Available: https://ieeexplore.ieee.org/document/9322355/

[10] M. C. Moroglu, H. M. Gursu, F. Clazzer, and W. Kellerer, "Short Frame Length Approximation for IRSA," *IEEE Wireless Communications Letters*, vol. 2337, no. c, pp. 10–13, 2020.

[11] S. Saha, V. B. Sukumaran, and C. R. Murthy, "On the Minimum Average Age of Information in IRSA for Grant-free mMTC," *IEEE Journal on Selected Areas in Communications*, vol. 8716, no. c, pp. 1–1, 2021. [Online]. Available: https://ieeexplore.ieee.org/document/9376691/

[12] D. Zhai, Y. Lu, R. Shi, and Y. Ji, "Large-scale micro-power sensors access scheme based on hybrid mode in iot enabled smart grid," in *2022 7th International Conference on Signal and Image Processing (ICSIP)*, 2022, pp. 719–723.

[13] J. Shang, W. Xu, Z. Zhang, Y. Fan, and J. Lin, "Reliable random access for decentralized uav networks based on raptor codes," *IEEE Internet of Things Journal*, vol. 8, no. 22, pp. 16 571–16 584, 2021.

[14] M. Shirvanimoghaddam, M. Dohler, and S. J. Johnson, "Massive multiple access based on superposition raptor codes for cellular m2m communications," *IEEE Transactions on Wireless Communications*, vol. 16, no. 1, pp. 307–319, 2017.

[15] Y. Xie, H. Ding, H. Jiang, and Y. Chen, "Enhanced coded random access for industrial internet of things," *IEEE Internet of Things Journal*, vol. 9, no. 5, pp. 3968–3981, 2022.

[16] V. C. Gungor, B. Lu, and G. P. Hancke, "Opportunities and challenges of wireless sensor networks in smart grid," *IEEE Transactions on Industrial Electronics*, vol. 57, no. 10, pp. 3557–3564, 2010.

[17] M. Centenaro, L. Vangelista, A. Zanella, and M. Zorzi, "Long-range communications in unlicensed bands: the rising stars in the iot and smart city scenarios," *IEEE Wireless Communications*, vol. 23, no. 5, pp. 60–67, 2016.

[18] A. Ahmed, M. Y. Arafat, M. M. Hossain, M. Abdelgawad, and J. H. Cui, "A survey of low power wide area network technologies for iot applications," *IEEE Internet of Things Journal*, vol. 4, no. 6, pp. 3044–3058, 2017.

[19] Y. Bourdena, A. K. Lalov, and P. Popovski, "Wireless communications with unmanned aerial vehicles: opportunities and challenges," *IEEE Communications Magazine*, vol. 55, no. 10, pp. 36–42, 2017.

[20] Y. Saleem, N. Crespi, M. H. Rehmani, and R. Copeland, "Internet of Things-Aided Smart Grid: Technologies, Architectures, Applications, Prototypes, and Future Research Directions," *IEEE Access*, vol. 7, pp. 62 962–63 003, 2019. [Online]. Available: https://ieeexplore.ieee.org/document/8701687/

[21] B. S. Chaudhari and M. Zennaro, *Introduction to low-power wide-area networks*. INC, 2020. [Online]. Available: http://dx.doi.org/10.1016/B978-0-12-818880-4.00001-6

[22] M. Kaveh and M. R. Mosavi, "A Lightweight Mutual Authentication for Smart Grid Neighborhood Area Network Communications Based on Physically Unclonable Function," *IEEE Systems Journal*, vol. 14, no. 3, pp. 4535–4544, sep 2020. [Online]. Available: https://ieeexplore.ieee.org/document/9036056/

[23] Jinho Choi, K. Lee, Yonggu Lee, and Nam Yul Yu, "Secure compressive random access for meter reading in smart grid using multi-antenna access point," in *2016 IEEE International Conference on Smart Grid Communications*

(SmartGridComm).   IEEE, nov 2016, pp. 116–121. [Online]. Available: http://ieeexplore.ieee.org/document/7778748/

[24] I. C. Society, *IEEE Standard for Low Rate Wireless Networks*.   IEEE, 2020, vol. 2020.

[25] IEEE, "Ieee standard communication delivery time performance requirements for electric power substation automation," *IEEE Std 1646-2004*, pp. 1–36, Feb 2005.

[26] K. Chan, J. Babiarz, and F. Baker, "Configuration Guidelines for DiffServ Service Classes," IETF, Tech. Rep., aug 2006. [Online]. Available: http://tools.ietf.org/pdf/rfc4594.pdf

[27] International Telecommunication Union - ITU, "G.114 - One-way transmission time," *ITU-T*, pp. 1–20, 2003. [Online]. Available: https://www.itu.int/rec/T-REC-G.114-200305-I/en

[28] International Telecommunication UnionTU - I, "G.107 : The E-model: a computational model for use in transmission planning," *ITU-T*, 2014.

[29] Y. Hu, M. Donnelly, T. Helmer, H. Tram, K. Martin, M. Govindarasu, R. Uluski, and M. Cioni, "Naspinet specification - an important step toward its implementation," in *Proceedings of the 2010 43rd Hawaii International Conference on System Sciences*, ser. HICSS '10.   Washington, DC, USA: IEEE Computer Society, 2010, pp. 1–9. [Online]. Available: http://dx.doi.org/10.1109/HICSS.2010.284

[30] J. G. Deshpande, E. Kim, and M. Thottan, "Differentiated services QoS in smart grid communication networks," *Bell Labs Technical Journal*, vol. 16, no. 3, pp. 61–81, dec 2011. [Online]. Available: http://ieeexplore.ieee.org/lpdocs/epic03/wrapper.htm?arnumber=6770300

[31] Z. Ma, M. Xiao, Y. Xiao, Z. Pang, H. V. Poor, and B. Vucetic, "High-reliability and low-latency wireless communication for internet of things: Challenges, fundamentals, and enabling technologies," *IEEE Internet of Things Journal*, vol. 6, no. 5, pp. 7946–7970, 2019.

[32] G. Group, "Nr, physical channels and modulation: 3gpp specification # 38.211," 3GPP Group, Technical specification (TS) Release 15, 2018.

[33] J. Vihriälä, A. A. Zaidi, V. Venkatasubramanian, N. He, E. Tiirola, J. Medbo, E. Lähetkangas, K. Werner, K. Pajukoski, A. Cedergren, and R. Baldemair, "Numerology and frame structure for 5g radio access," in *2016 IEEE 27th Annual International Symposium on Personal, Indoor, and Mobile Radio Communications (PIMRC)*, 2016, pp. 1–5.

[34] M. Berioli, G. Cocco, G. Liva, and A. Munari, "Modern Random Access Protocols," *Foundations and Trends® in Networking*, vol. 10, no. 4, pp. 317–446, 2016. [Online]. Available: http://www.nowpublishers.com/article/Details/NET-047

[35] R. A. Kennedy and L. E. Miller, "Packet switching in radio channels: Part ii–the hidden terminal problem in carrier sense multiple-access and the busy-tone solution," *IEEE Transactions on Communications*, vol. 23, no. 9, pp. 995–1005, 1975.

[36] D. G. Daut and R. A. Shorey, "Analysis of a random-access scheme for satellite networks," *IEEE Transactions on Communications*, vol. 29, no. 11, pp. 1660–1671, 1981.

[37] C. Eklund and A. Rahelić, "Packet radio networks with slotted ALOHA: Multi-access performance," *IEEE Transactions on Communications*, vol. 34, no. 6, pp. 523–530, 1986.

[38] J. Huang and M. van der Schaar, "Compressive sensing for efficient and reliable random access in machine-to-machine communications," *IEEE Transactions on Wireless Communications*, vol. 14, no. 1, pp. 190–203, 2015.

[39] T. V. Le and H. V. Poor, "A probabilistic method for medium access control in wireless networks," *IEEE Transactions on Information Theory*, vol. 65, no. 10, pp. 6446–6471, 2019.

[40] H. Kim, J. Ha, and B. Clerckx, "On the throughput analysis of slotted ALOHA for massive machine-type communications," *IEEE Transactions on Communications*, vol. 68, no. 6, pp. 3717–3728, Jun. 2020.

[41] W. U. Hassan, A. M. A. M. Nassar, M. M. Alwakeel, and M. Bennis, "Distributed power control in slotted ALOHA networks: A mean-field game perspective," *IEEE Transactions on Wireless Communications*, vol. 19, no. 6, pp. 3874–3888, Jun. 2020.

[42] T. N. Sunita and A. Bharathi Malakreddy, "A Survey of MTC Traffic Models in Cellular Network," in *International Conference on Computer Networks and Communication Technologies*, ser. Lecture Notes on Data Engineering and Communications Technologies, S. Smys, R. Bestak, J. I.-Z. Chen, and I. Kotuliak, Eds. Singapore: Springer Singapore, 2019, vol. 15, pp. 681–693. [Online]. Available: http://link.springer.com/10.1007/978-981-10-8681-6_62

[43] J. Navarro-Ortiz, P. Romero-Diaz, S. Sendra, P. Ameigeiras, J. J. Ramos-Munoz, and J. M. Lopez-Soler, "A Survey on 5G Usage Scenarios and Traffic Models," *IEEE Communications Surveys & Tutorials*, vol. 22, no. 2, pp. 905–929, 2020. [Online]. Available: https://ieeexplore.ieee.org/document/8985528/

[44] H. M. Gursu, M. C. Moroglu, M. Vilgelm, F. Clazzer, and W. Kellerer, "System Level Integration of Irregular Repetition Slotted ALOHA for Industrial IoT in 5G New Radio," *IEEE International Symposium on Personal, Indoor and Mobile Radio Communications, PIMRC*, vol. 2019-September, pp. 2–8, 2019.

[45] H. M. Gursu, W. Kellerer, and C. Stefanovic, "On Throughput Maximization of Grant-Free Access with Reliability-Latency Constraints," in *ICC 2019 - 2019 IEEE International Conference on Communications (ICC)*, vol. 2019-May. IEEE, may 2019, pp. 1–7. [Online]. Available: https://ieeexplore.ieee.org/document/8761270/

[46] A. Mengali, R. De Gaudenzi, and C. Stefanovic, "On the Modeling and Performance Assessment of Random Access with SIC," *IEEE Journal on Selected Areas in Communications*, vol. 36, no. 2, pp. 292–303, 2018.

[47] E. Dahlman, S. Parkvall, and J. Sköld, *5G NR: the Next Generation Wireless Access Technology*, 1st ed. Elsevier, 2018. [Online]. Available: https://linkinghub.elsevier.com/retrieve/pii/C20170013472

[48] P. Kansal and A. Bose, "Bandwidth and latency requirements for smart transmission grid applications," *IEEE Transactions on Smart Grid*, vol. 3, no. 3, pp. 1344–1352, 2012.

[49] R. Sahner, K. S. Trivedi, and A. Puliafito, "Reliability and Availability Models," in *Performance and Reliability Analysis of Computer Systems*. Boston, MA: Springer US, 1996, pp. 27–46. [Online]. Available: http://link.springer.com/10.1007/978-1-4615-2367-3{_}2

[50] I. N. A. Ramatryana and K. Anwar, "Raptor decoding for high overloaded wireless super-dense networks," *2017 8th International Workshop on Signal Design and Its Applications in Communications, IWSDA 2017*, pp. 29–33, 2017.

[51] A. Shokrollahi, "Raptor codes," *IEEE Transactions on Information Theory*, vol. 52, no. 6, pp. 2551–2567, jun 2006. [Online]. Available: http://ieeexplore.ieee.org/document/1638543/

[52] W. Wang, X. Li, and H. Chen, "Design of raptor codes based on interleaver optimization for the internet of things," *IET Communications*, vol. 13, no. 5, pp. 651–657, 2019.

[53] 3GPP, "3gpp ts 38.214 v16.1.0," 2019, 5G Radio Access Network (RAN) Standard. [Online]. Available: https://www.3gpp.org/ftp//Specs/archive/38_series/38.214/

[54] H. Chen, X. Li, W. Wang, and L. Guan, "A new raptor code-based parallel data transmission method for iot," in *2020 IEEE 91st Vehicular Technology Conference (VTC2020-Spring)*, 2020, pp. 1–5.

[55] Q. Xu, X. Chen, Q. Guo, P. Liu, and Z. Qin, "Design of an efficient and reliable leo satellite communication system based on raptor codes," in *2018 IEEE International Conference on Communications Workshops (ICC Workshops)*, 2018, pp. 1–6.

[56] M. Li, X. Lin, L. Huang, Y. Li, and H. Zhang, "Optimized frame length for slotted aloha systems: A stochastic geometry perspective," *IEEE Transactions on Wireless Communications*, vol. 18, no. 4, pp. 2184–2197, 2019.

[57] S. Datta, S. Das, D. Saha, and S. Chattopadhyay, "Performance analysis of random access protocols for machine type communication: A survey," *IEEE Communications Surveys & Tutorials*, vol. 22, no. 1, pp. 552–588, 2020.

[58] J. Wang, C. Liu, H. Qian, and X. S. Shen, "Efficient decoding algorithms for random access in machine-to-machine communications," *IEEE Transactions on Vehicular Technology*, vol. 70, no. 2, pp. 1514–1526, 2021.

[59] P. Zhang, Q. Zhan, C. Yang, and H. Xu, "An efficient channel access scheme for cellular m2m communications: From code to signal design," *IEEE Transactions on Communications*, vol. 69, no. 3, pp. 1659–1670, 2021.

[60] Y. Beytur and U. Cagri Guven, "Random access in cellular networks with random repetition slotted aloha," *IEEE Transactions on Wireless Communications*, vol. 19, no. 3, pp. 1773–1787, 2020.

[61] J. Niu, J. Chen, L. Li, P. Fan, and J. Wang, "Congestion control for machine-to-machine communications in cellular networks," *IEEE Journal on Selected Areas in Communications*, vol. 30, no. 3, pp. 559–570, 2012.

[62] A. Sridharan and S. Diggavi, "Practical lt codes for general network topologies," *IEEE Transactions on Information Theory*, vol. 54, no. 6, pp. 2723–2731, 2008.

[63] T. Richardson and R. Urbanke, *Modern Coding Theory*. Cambridge University Press, 2008.

[64] J. Sun, R. Liu, Y. Wang, and C. W. Chen, "Irregular Repetition Slotted ALOHA with Priority (P-IRSA)," in *2016 IEEE 83rd Vehicular Technology Conference (VTC Spring)*, vol. 2016-July. IEEE, may 2016, pp. 1–5. [Online]. Available: http://ieeexplore.ieee.org/document/7504302/

[65] S. Bolognani, A. Zanella, L. Vangelista, and M. Zorzi, "Smart grid communications: Overview of research challenges, solutions, and standardization activities," *IEEE Communications Surveys & Tutorials*, vol. 15, no. 1, pp. 21–38, 2013.

[66] K. Tse and W. Wu, "Modelling of power grids using complex network theory," in *2018 IEEE Power & Energy Society General Meeting (PESGM)*, 2018, pp. 1–5.